

Jet pinch-off and drop formation in immiscible liquid–liquid systems

D. R. Webster, E. K. Longmire

Abstract The behavior of glycerin–water jets flowing into immiscible ambients of Dow Corning 200 fluid was investigated using laser induced fluorescence (LIF). Undistorted images were obtained by matching the index of refraction of the fluids. A sinusoidal perturbation was superposed on the flow to phase lock the drop formation. The forcing frequency dramatically affected the size, spacing, and number of drops that formed within a forcing cycle and the angle between drops and the jet interface just before pinch-off. Two fluid combinations were studied with similar density ratios, but viscosity ratios differing by a factor of 20. The viscosity ratio affected the jet stability as well as pinch-off angles and drop size.

1

Introduction

A fundamental phenomenon in fluid dynamics involves changes in the topology of interfaces between nominally immiscible fluids. Common examples of topological changes are pinch-off of a continuous jet into droplets and droplet reconnection. Because of the importance of such flows, it is desirable to develop accurate models for mixing, separation, and reaction rate that are applicable to a wide variety of flow geometries and parameters. Before such models can be developed, however, it is crucial to understand the dynamics of topological transitions.

The dynamics of topological transitions are difficult to characterize for several reasons. First, a number of fluid

properties, such as density, viscosity, interfacial tension, and diffusivity, may play a role in the transition process. Second, flow parameters, such as the dominant length and velocity scales, affect the balance of inertial, buoyant, viscous, and interfacial tension forces that determine the timing and nature of transitions. In particular, the transitions typically result from a competition between flow instabilities due to shear or buoyancy, and stabilizing influences due to interfacial tension and viscosity. Finally, the transitions themselves usually occur over very short time scales relative to local flow time scales. Therefore, the transitions are often difficult to observe experimentally. The goal of this study is to investigate the fundamental behavior of jet pinch-off and the resulting drop formation.

The flow of a liquid jet into a second ‘immiscible’ liquid has been studied by a number of investigators due to its occurrence in many chemical processing systems. (For example, see Scheele and Meister 1968; Meister and Scheele 1969a, b; Skelland and Johnson 1974; Kitamura et al. 1982; Richards and Scheele 1985; Tadrif et al. 1991; Richards et al. 1994.) Meister and Scheele performed experiments on a large number of fluid combinations in order to determine empirical relationships for jet length and resulting drop size based on input parameters. Skelland and Walker (1989) determined similar relationships that included the effects of surfactants. One important trend shown by these experiments was the influence of Reynolds number on the ‘mode’ of the flow downstream. In general, for low Reynolds numbers, droplets form at and detach from the jet outlet. As Re is increased, the injected fluid forms a jet that develops axisymmetric instabilities and eventually pinches off at a finite length. Above a certain maximum Reynolds number, three-dimensional instabilities occur, and the jet length begins to decrease. The Re range corresponding to each flow mode depends significantly on the other system parameters.

A number of studies have focused on the detailed behavior of liquid pinch-off or drop formation in air (see recent experiments by Zhang and Basaran 1995, for example). In theoretical work, the outer fluid (air) is assumed to have no influence on the pinch-off process. Recent examples of this work include boundary integral computations by Brenner et al. (1997) and Cristini et al. (1998). Experiments by Brenner et al. (1997) showed that the viscosity of the inner fluid had a strong effect on the shape of the pinch-off region when drops formed in a gravity-driven flow with very small inertia. As inner fluid viscosity was increased (above the viscosity of water), the

Received: 28 January 1999/Accepted: 20 January 2000

D. R. Webster (✉)
School of Civil and Environmental Engineering,
Georgia Institute of Technology, Atlanta,
GA 30332-0355, USA
e-mail: dwebster@ce.gatech.edu

E. K. Longmire
Department of Aerospace Engineering and Mechanics,
University of Minnesota, Minneapolis,
MN 55455, USA

This work was supported by the National Science Foundation under grant CTS-9457014 and the Engineering Research Program of the Office of Basic Energy Sciences at the Department of Energy under grant DE-FG02-98ER1-4869. We wish to thank Derek Gefroh and Dave Hultman for construction of the facility and Dr. Harry Vinagre and Professor Dan Joseph for use of the spinning drop tensiometer.

angle between the plane normal to the flow axis and the upstream fluid interface increased from about 80° to nearly 90° . As the viscosity was increased further, the angle between this plane and the downstream fluid interface increased from about 8° to 80° . In a recent paper, Lister and Stone (1998) examined the break-up of strained dumbbell shapes where the inner and outer fluids had matched viscosity. They found that non-negligible viscosity in the outer fluid eliminated the influence of inertia within the inner flow. The pinch-off process and shape were instead dominated by viscous and capillary effects. In the matched viscosity case, the shape on either side of the pinch-off region was conical, and the two angles described above were 78° and 6° (the smaller angle corresponded with a large drop pinching off of a smaller neck). Experiments have also examined the shape of the fluid interface during break-up of single droplets subjected to plane strain (see the review by Stone 1994).

The study described herein is motivated by the general problem of quantifying and understanding the detailed dynamics of the pinch-off process when a number of fluid or flow parameters might be important, including the viscosity of the outer fluid. The jet flow is chosen for its relative simplicity as well as its practical significance. A laser sheet visualization method is used to observe pinch-off and drop formation dynamics. As described below, we employ a forcing method in order to make the pinch-off and drop formation process highly repeatable. In addition, we apply an index of refraction matching technique in order to visualize the interior of the flow and shape of the interface without distortion, thus revealing narrow gaps and any 'concave' curvature or 'overturning' with respect to the inner fluid.

2 Experimental description

The experiments were performed in the closed loop facility depicted in Fig. 1. The facility tank had a 203-mm^2 cross-section and 560-mm height. The tank was filled with a combination of the immiscible fluids. The upper 200 mm of the tank contained the lighter, less dense fluid, while the remainder was filled with the heavier fluid. The heavier fluid was drawn from the bottom of the tank and driven through the flow loop by a $1/35\text{-hp}$ magnetic-drive pump. A needle valve controlled the flow rate, which was measured with a rotameter. Before entering the tank facility, the flow passed through a honeycomb straightening section and a $16.5:1$ axisymmetric area contraction. The diameter of the submerged exit nozzle was 10 mm .

A piston-driven forcer was used to impose a regular sinusoidal oscillation on the nozzle exit velocity. The si-

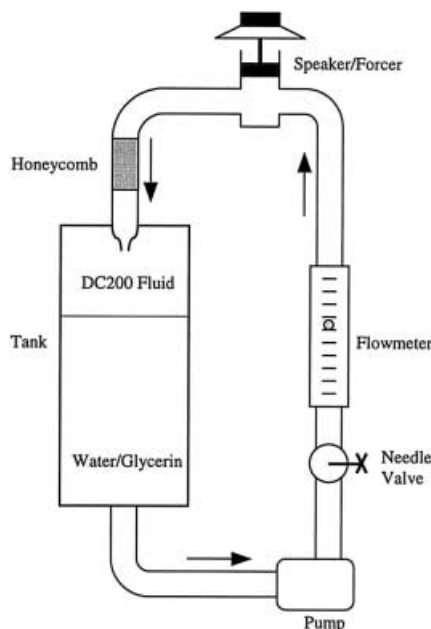


Fig. 1. Jet flow facility

nusoidal signal was generated with a National Instruments board installed in a Macintosh computer. The signal was amplified and connected to a standard audio speaker. A thin rod connected the speaker to a sealed piston assembly housed in a cylindrical reservoir in the flow path. The signal frequency and amplitude were varied with the computer and amplifier, respectively.

The jet column and drops were visualized using laser-induced fluorescence (LIF). A small quantity of Rhodamine 6G dye (less than 0.03 g/l) was added to the jet fluid. When excited by light in the green wavelength range, this dye fluoresces in the yellow/orange wavelength range. An illumination sheet was generated with a pulsed Nd:YAG laser ($\lambda = 532\text{ nm}$) and a combination of spherical and cylindrical lenses. The pulse strength was approximately 50 mJ , and the duration was 7 ns . The laser sheet thickness was less than 1 mm in the region of flow examined.

All images were captured with a Kodak DCS 420M digital camera. The pixel array dimension was 1012 by 1524 , and the pixel depth was 8 bits. Nikon AF Micro-Nikkor 105-mm and 60-mm lenses were employed on the camera. The timing of the laser and camera was controlled relative to the sinusoidal forcing signal with the Macintosh computer. By precisely timing the laser firing, individual phases within the forcing cycle could be imaged and repeated.

Table 1. Fluid properties

Fluid combination		ρ (kg/m^3)	ν (cS)	μ (cP)	n_D	ρ_i/ρ_o	μ_i/μ_o
1						1.18	0.152
<i>o</i>	Dow corning 200 fluid	960	50	48	1.403		
<i>i</i>	Water-glycerin (53.4% by weight)	1135	6.4	7.3	1.403		
2						1.17	0.0077
<i>o</i>	Dow corning 200 fluid	970	1000	970	1.404		
<i>i</i>	Water-glycerin (54.0% by weight)	1136	6.6	7.5	1.404		

3

Fluid properties

Two fluid combinations were employed in this study. In both combinations, one fluid was a water-glycerin mixture, and the other was a Dow Corning 200 fluid. The fluid properties for the two combinations are shown in Table 1, where ρ is fluid density, ν is kinematic viscosity, μ is dynamic viscosity, and n_D is index of refraction. The jet and ambient fluid are denoted with i and o , respectively.

The proportion for the water-glycerin mixture was chosen in order to match the index of refraction of the DC200 fluid. Matching the index of refraction was critically important for capturing clear images of the flow. If the index of refraction was not matched, the three-dimensional interface between the fluids adversely distorted the image. When matched, both fluids appear transparent, and the camera images the fluoresced light without distortion.

The interfacial tension was measured to be 29 mN/m using a spinning drop tensiometer (Joseph et al. 1992) for fluid combination 1. Hence the non-dimensional Bond number, $Bo = \Delta\rho g D^2 / \sigma$, was approximately 6, where $\Delta\rho$ is the density difference between fluids, g is the gravitational constant, D is the nozzle diameter, and σ is the interfacial tension.

The remaining parameters chosen to characterize the flow were the density ratio, the viscosity ratio, a Reynolds number based on the jet flow and fluid properties, a Froude number, and a Strouhal number (for forced flow):

$$\frac{\rho_i}{\rho_o}, \frac{\mu_i}{\mu_o}, Re = \frac{\rho_i U_e D}{\mu_i}, Fr = \frac{U_e \sqrt{\rho_i}}{\sqrt{\Delta\rho g D}}, St = \frac{f D}{U_e}$$

where U_e is the jet exit velocity, and f is the forcing frequency. The Reynolds number represents the ratio of inertial to viscous forces, the Froude number represents the ratio of inertial to buoyant forces, and the Bond number represents the ratio of buoyant to interfacial tension forces. For the flow conditions chosen, the effects of inertia, gravity, and interfacial tension were all significant.

In this study, the effects of forcing frequency (St) and viscosity ratio were examined. Therefore, St was varied using fluid combination 1 while holding the other parameters constant. In addition, the Reynolds and Froude numbers were held constant, while the viscosity ratio was varied. It should be noted that the density ratio was essentially the same for each fluid combination, but the viscosity ratio varied by more than an order of magnitude.

4

Results

4.1

Fluid combination 1

The facility was tested over a range of velocities in order to characterize the type and location of pinch-off that occurred. In general, the Froude number was small enough that gravitational effects were significant. Thus, upon exiting the nozzle the natural (unforced) jet accelerated and consequently decreased in cross-sectional area. For $Re > 50$ ($Fr > 0.26$), the jet did not pinch off before reaching the interface between glycerin-water and DC200

fluid reservoirs. At $Re = 34$ ($Fr = 0.17$), the pinch-off location was approximately $15 D$ below the nozzle. As the flow rate was decreased, the pinch-off position moved upstream until a ‘dripping’ mode occurred at $Re = 11$ ($Fr = 0.06$) characterized by drops forming adjacent to the nozzle, detaching, and propagating downstream.

Four images of unforced flow at $Re = 16$ ($Fr = 0.08$) are shown in Fig. 2. In these and subsequent visualization images, the flow moves from right to left, and gravity is directed toward the left. Note that the nozzle exit is slightly upstream of the right edge of each photograph. Figure 2a shows a pattern of drop formation with drops of relatively constant diameter (approximately $0.8 D$). Figure 2b and c show a range of drop size and spacing indicating more erratic pinch-off. The size of the largest drops is similar to those in Fig. 2a. Note the axisymmetric instability waves on the interface in Fig. 2b. The instability wave appears to contain several wavelengths, which explains the possibility for variation in size and spacing of the resulting drops.

At this Reynolds number, the jet was unstable to mild perturbations, such as firmly tapping the side of the tank. Such a perturbation could shift the flow to the dripping mode shown in Fig. 2d. The flow also contained some degree of hysteresis. For example, if the flow rate was increased to achieve $Re = 16$, the drop mode resulted, but if the flow rate was decreased to achieve the same Re , the jet mode resulted.

Perturbing the jet with a single forcing frequency causes the pinch-off location to move upstream closer to the nozzle. In the forced cases described below, the amplitude of the forcing signal was chosen as the minimum required to stabilize various pinch-off modes such that the mode repeated with precision once every forcing cycle.

Two images of the jet forced at $St = 3.1$ (10 Hz) are shown in Fig. 3. The unforced jet at these conditions ($Re = 50$ and $Fr = 0.26$) yields a stable jet column with a diameter of $0.4 D$ at a distance of $20 D$ downstream of the nozzle exit (the location of the reservoir interface). The forcing creates regular axisymmetric instability waves on

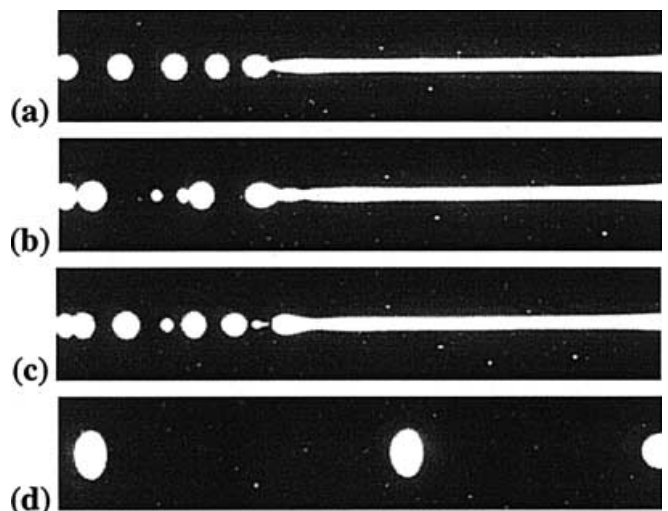


Fig. 2. Natural jet at $Re = 16$, $Fr = 0.08$, fluid combination 1. Length of each image is $17.5 D$

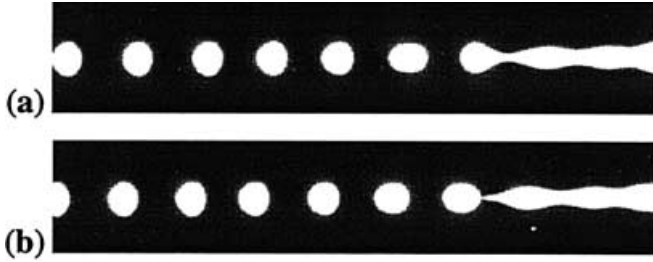


Fig. 3. Forced flow at $Re = 50$, $Fr = 0.26$, $St = 3.1$, fluid combination 1. Length of each field is $18.1 D$

the jet column, which cause the jet to pinch off approximately $5.5 D$ below the nozzle. The exact pinch-off location is a sensitive function of the forcing amplitude. In Fig. 3b, pinch-off is imminent. At this frequency, a single drop forms during each forcing cycle. The drop size and spacing is uniform, and the drops do not interact before they eventually impact the flat interface downstream. The nominal diameter of each drop is approximately $0.9 D$, and the drop propagation velocity is $6.2 U_e$.

Immediately after pinch-off, each drop has the shape of a prolate spheroid. However, as a given drop propagates downstream, its shape develops into an oblate spheroid with flattened rear. The drop Reynolds number based on drop diameter, d , propagation speed, V , and ambient fluid properties is 40 ($Re_{\text{drop}} = \rho_o V d / \mu_o$). Isolated spheres at this Re_{drop} are known to develop an attached separation region containing small, relatively steady recirculation zones (Batchelor 1967). Such a separation behind a drop moving at a steady velocity would yield a lower pressure on the upstream end of the drop than on the downstream end. This suggests that a local pressure maximum caused by the external flow is not responsible for the flattening of the surface. In fact, flows of isolated drops in a liquid surrounding at similar Re yield shapes that are flattened on the downstream side (see Clift et al. 1978). The most likely causes of the upstream ‘flattening’ are residual stresses due to interfacial tension and residual velocities associated with the pinch-off process. In the experiments described, the drop propagation could not be observed over a long enough distance to ascertain whether the shape would exhibit low frequency oscillations.

In Fig. 4, the pinch-off process is observed in closer detail. Since the forcing causes the pinch-off to repeat with precision once every forcing cycle, a series of phase-locked images was used to reconstruct a pinch-off sequence (thus, each image shown depicts a separate pinch-off event). The phase difference between neighboring images is 10° representing a time difference of 2.78 ms. The twenty images thus span slightly more than half of a forcing cycle. At the beginning of the sequence, the shape of the axisymmetric jet column instability appears nearly sinusoidal. As time advances, however, the tip evolves into a prolate spheroid. At the junction of the developing spheroid and the jet column, the radius of curvature begins to decrease until it reaches an extremely small scale. The jet column necks down into a pointed cone that eventually pinches off.

If the drop volume is estimated by projecting around the drop circumference, the volume increases by more

than 10% from the phase at top left to the phase 60° later, implying a locally high velocity and significant flow rate in the jet stem. In the subsequent phases before pinch-off, the drop does not grow appreciably, indicating a decrease in the flow rate within the stem.

The cone shape observed upstream of the pinch-off agrees fairly well with the computational results of Zhang and Stone (1997) who applied a boundary integral method to study drop formation at the end of a capillary tube. The shape of the drop shortly before pinch-off differs, however. In the computation, the upstream end of the drop was pointed as pinch-off approached, resembling a tear drop. In the current images, the drop has a rounded end connected to the jet stem (refer to the images at bottom left of Fig. 4). The cone shape also agrees qualitatively with the boundary integral algorithm results of Cristini et al. (1998) and Lister and Stone (1998) for strained drops.

It is interesting to observe the recoil of the jet tip, which is shown in the right-hand column of images. Once the drop separates from the jet column, the position of the jet tip remains at a fixed axial position in the ensuing phases shown (over 90° of the forcing cycle). Compare the image just after pinch-off to the last image shown at bottom right. The drop advects forward over time, but the tip does not. The axial velocity of the jet tip is therefore close to zero for a significant portion of the forcing cycle. During this time, the tip shape changes significantly as jet fluid moves downward from above, and interfacial tension acts to decrease the local curvature. In the last image, the tip has begun to resemble the prolate spheroid associated with the next drop. The temporary stagnation of the jet end and the gradual rounding of the tip must result from the upward interfacial tension force acting against the downward gravitational force.

In Fig. 5, three close-up views of the pinch-off region are shown. The prolate spheroid shape is evident in each image. The connection with the jet column becomes increasingly thin before it eventually pinches off (third image). In the second image, the minimum diameter shown is $180 \mu\text{m}$. As shown in Fig. 5, the angle defined by the drop and jet column connection is split into an upstream and downstream contribution, β_u and β_d . At this time, the angles were measured as 74° and 28° , respectively. Note that these angles (especially β_d) change as the stem shrinks.

In Fig. 5, one can observe a decrease in scattering intensity near the pinch-off position as well as elsewhere along the interface. It is likely that the reduced intensity results from the LIF visualization method. The gray zones typically occur where the laser sheet intersects jet regions of small thickness relative to the laser sheet thickness. For this reason, it is possible that the laser sheet excites relatively few dye molecules in these regions, too few to saturate those portions of the camera array.

4.2

Effect of forcing frequency

The frequency of the forcing strongly affected the drop formation and propagation dynamics. Figure 6 shows one complete forcing cycle for three Strouhal numbers at the same Reynolds and Froude numbers discussed above. In

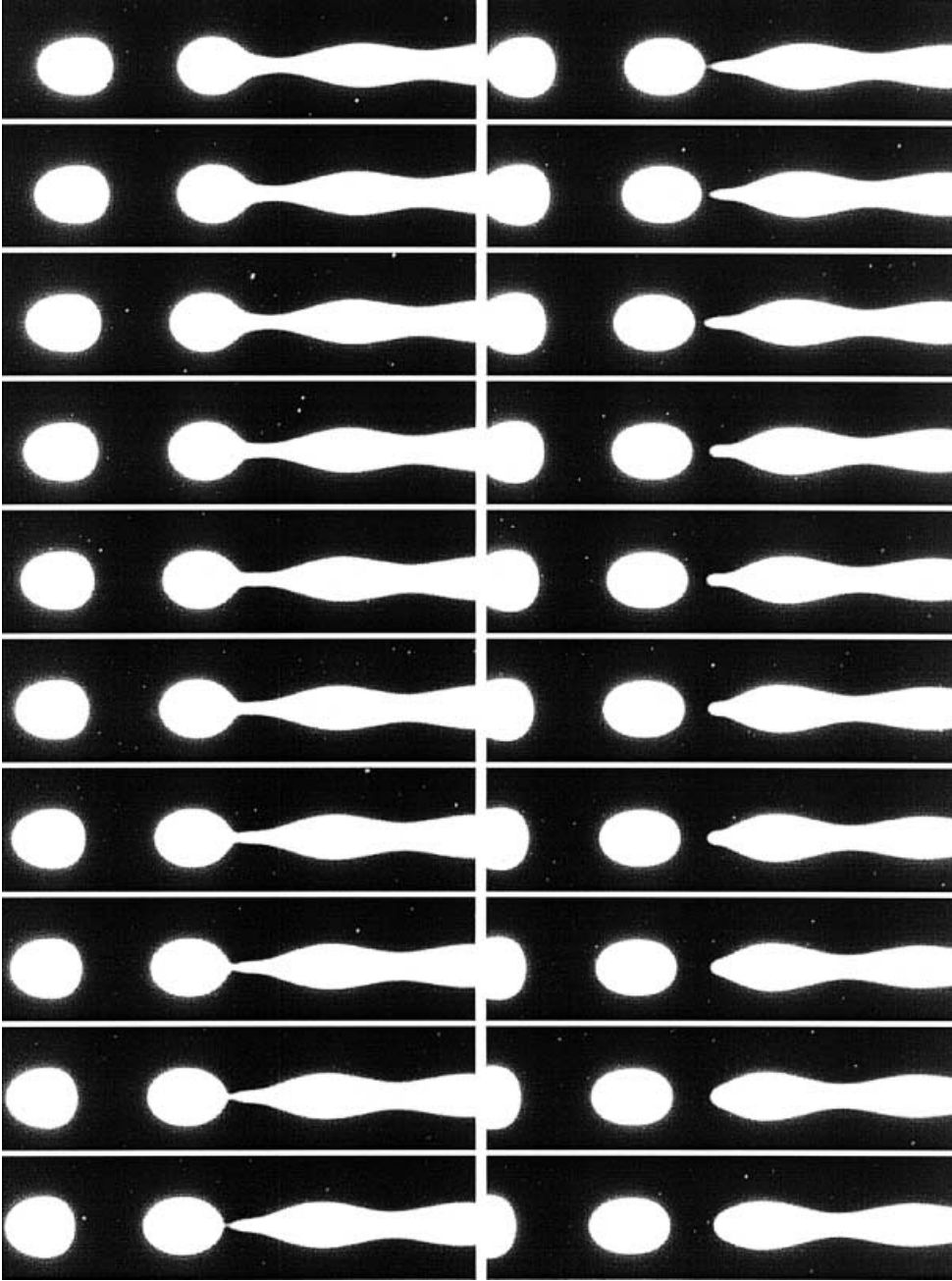


Fig. 4. Phase-locked reconstruction of jet pinch-off. Sequence proceeds top-to-bottom starting with the left-hand column. $Re = 50$, $Fr = 0.26$, $St = 3.1$, fluid combination 1. Length of each field is $6.5 D$

each case, the images are separated by 30° of the forcing cycle. The images in column (c) ($St = 3.1$) correspond to the same flow conditions shown in Fig. 4, where the first five images show additional flow phases. From viewing the entire forcing cycle, we see that after pinch-off the jet tip remains stationary for approximately 150° of the forcing cycle. During this portion of the cycle, the drop moves away from the stationary tip until it is located $0.6 D$ downstream. At this point, the jet tip begins moving downward again (see the second image in the sequence). During this stage, the tip velocity remains smaller than the drop velocity so that the gap increases to a value of $0.95 D$ by the time the trailing drop pinches off. This spacing is then maintained as the drops propagate downstream.

Halving the forcing frequency to $St = 1.6$ yielded a pair of drops for each forcing cycle (see Fig. 6b). During the

cycle, a large drop ($d \approx 0.95 D$) and a smaller drop ($d \approx 0.5 D$) pinch off at approximately 180° intervals. The existence of the drop pair suggests that the fundamental instability frequency of the jet is significantly higher than this forcing frequency. It also suggests that the local jet diameter mandates a maximum drop size. In this case, the volume of fluid associated with one cycle is twice that in the fundamental case discussed above. A single drop containing all of the fluid is evidently not possible, and the observed pair is formed instead. This can be understood physically by looking at the development of the larger drop in the pair: The drop evolves from the ‘thick’ portion of a wave imposed on the jet. The local diameter increases as the drop grows on the jet end. In the top figure of the sequence, the ratio of the drop diameter to the jet diameter upstream is quite large (≈ 3.8). At this point, the down-

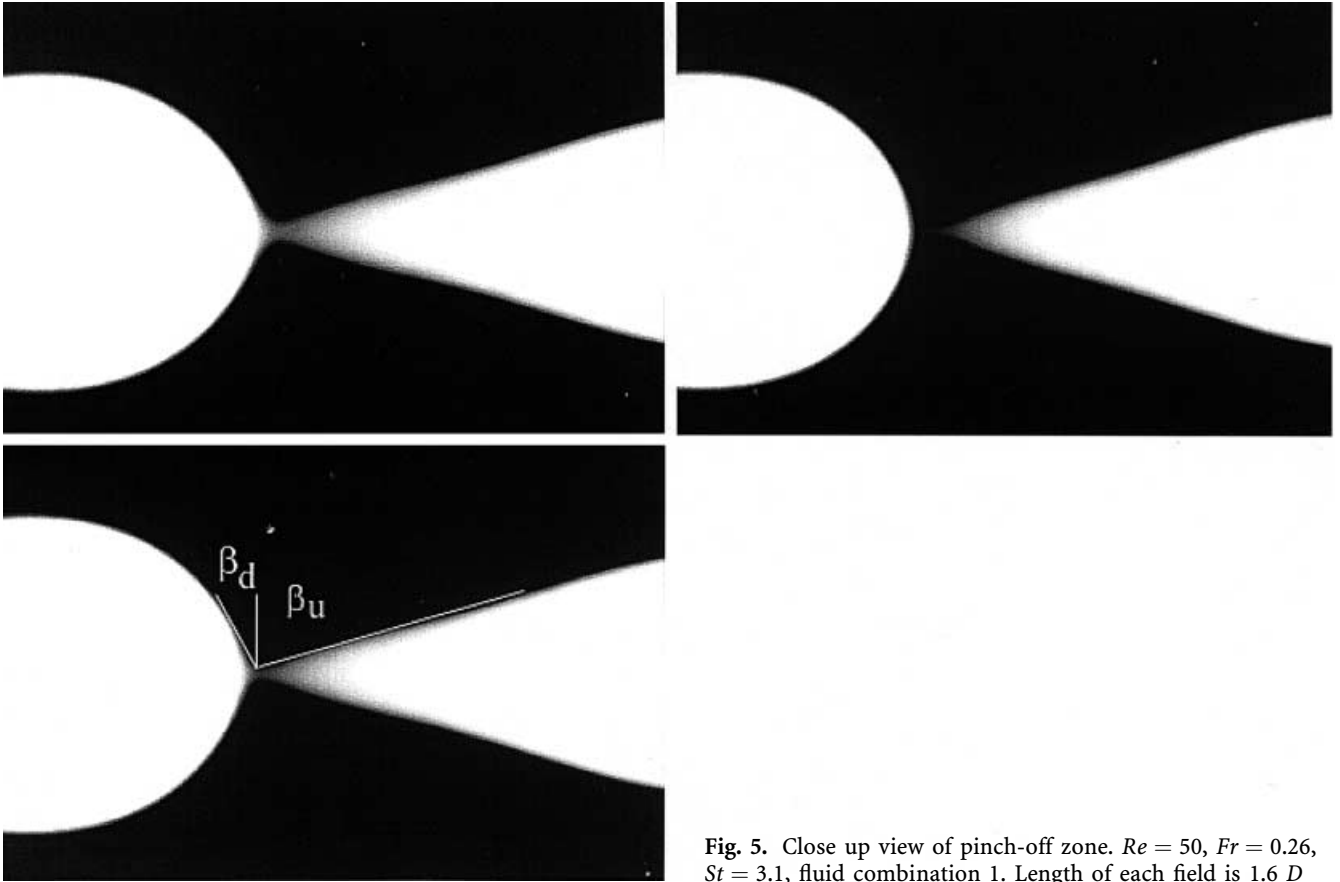


Fig. 5. Close up view of pinch-off zone. $Re = 50$, $Fr = 0.26$, $St = 3.1$, fluid combination 1. Length of each field is $1.6 D$

ward velocity of the drop becomes comparable to the downward velocity in the jet stem, so the drop begins to pinch off before a forcing cycle can be completed. Since the buoyant force on a drop scales with volume (i.e., d^3) and the drag force at low Re scales approximately with d , it is expected that a structure with larger diameter will eventually move faster than one with a smaller diameter, explaining the tendency of the large drop to accelerate and pinch off rather than to continue to grow.

This tendency is most likely reinforced by the sinusoidal velocity perturbation originally imposed on the flow. The temporal velocity variation at the jet exit causes a spatial velocity variation in the developing jet, and this variation encourages axisymmetric waves to grow in amplitude as the flow moves downstream. Over time, the 'thick' section of the wave increases in volume, and the narrow section decreases in volume. Considering the reference frame of a continuous wave, the thick section grows because high velocity fluid enters from upstream, while low velocity fluid exits downstream. From this simple argument, a maximum in streamwise velocity should occur approximately one-quarter wavelength upstream of a maximum in diameter. The velocity decreases with further upstream distance over half of a wavelength. When this zone of decreasing velocity approaches the drop, pinch-off is encouraged.

The scaling argument given above also explains the difference in propagation speed observed for the two drops in each pair. It can be seen that the larger drop

propagates much more quickly than the smaller one so that the larger drop catches up to and 'pushes' its companion. (A large drop pushing a smaller one is also observed in Fig. 2b for the natural case at $Re = 16$, $Fr = 0.08$.) In the forced case of Fig. 6b, the paired drops did not coalesce before they reached the bottom of the DC200 fluid reservoir. This suggests that the relative force between them was small, and that the drainage of DC200 fluid between the drops was slow. Studies on the coalescence of single drops at interfaces yield drainage times on the order of seconds, and the available travel time for the drop pair in the current study is only about one second (see Vijayan et al. 1975, for example).

Halving the forcing frequency again ($St = 0.8$) results in a series of five drops per forcing cycle. In order, the sizes of the drops that form are approximately $1 D$, $0.8 D$, $0.65 D$, $0.56 D$, and $0.4 D$. This case produced the largest drop size compared with the two previous cases. Again, the size of the largest drop appears to be limited by a complex balance of forces. In Fig. 6a, as pinch-off of the largest drop begins, the ratio of drop diameter to upstream jet diameter has grown to 2.4, which is less than that in the $St = 1.6$ case. The absolute diameter of this drop is larger, however, giving a greater relative importance to the downward gravitational force, and hence encouraging pinch-off. The diameter ratio preceding pinch-off decreases for the smaller drops in the cycle. The two smallest drops separate from the jet column together, briefly forming an elongated shape with a spherical head and

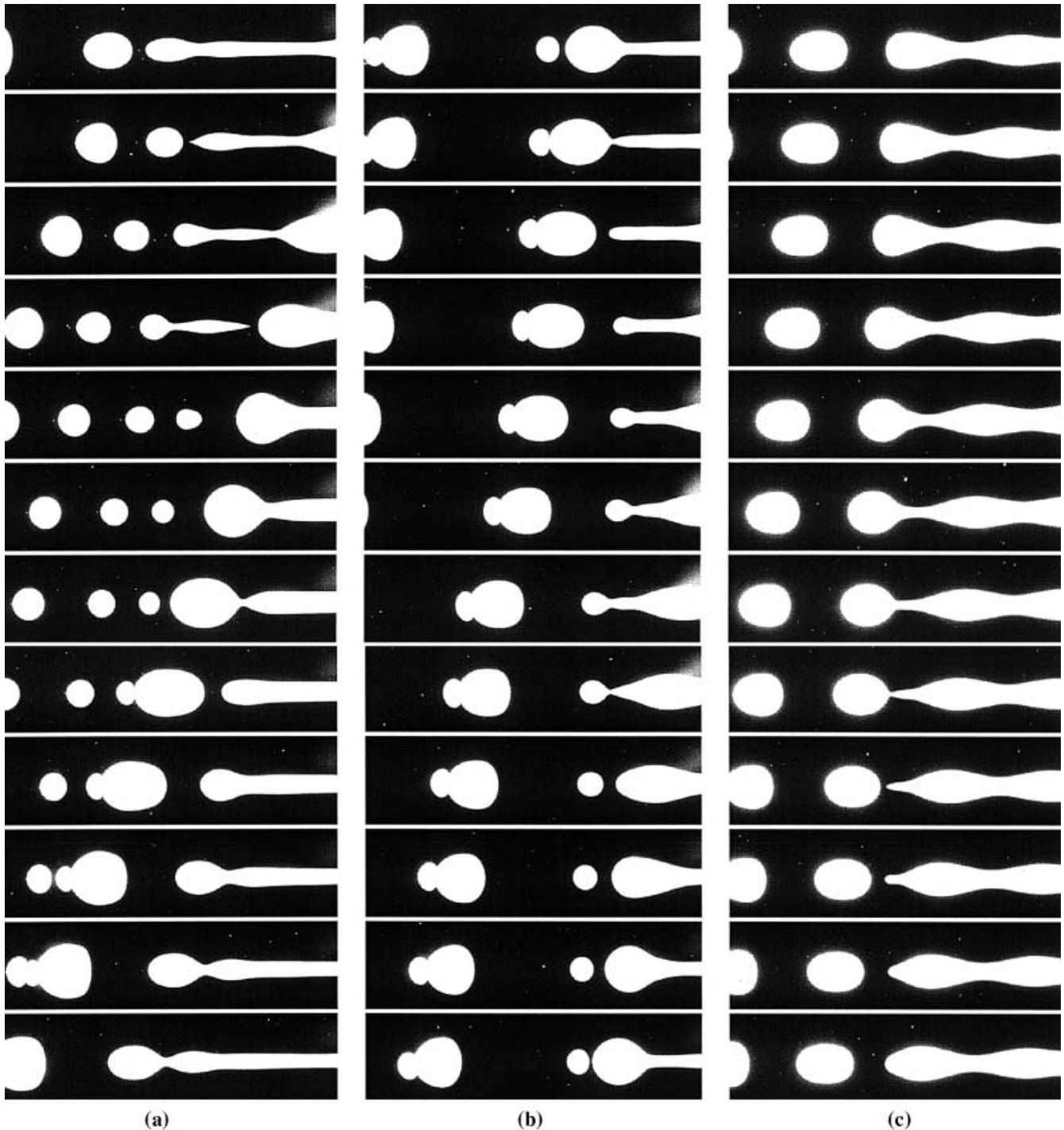


Fig. 6a-c. Phase locked reconstruction of pinch-off cycle for three Strouhal numbers: a $St = 0.8$, b $St = 1.6$, c $St = 3.1$. $Re = 50$, $Fr = 0.26$, fluid combination 1. Length of field for a and b is $6.7 D$ and for c is $6.5 D$

narrow tail. The tail then pinches off from the head to form the smallest drop. This phenomenon appears similar to 'satellite' formation observed in previous studies of dripping or straining flows in air. For example, Brenner et al. (1997) observed a similar (very small) structure that formed upstream of a pinching water drop.

Again in this forcing case, the largest drop moved the fastest so that it eventually caught up with two smaller downstream drops and pushed both of them forward. Again, the drops maintained distinct shapes and did not

coalesce before they reached the reservoir interface. The upstream flattening of the largest drop in this case appears stronger than that observed in the drops formed at higher frequencies. It is unknown whether the flattening is caused solely by effects near the upstream end of the drop or whether it is enhanced by the collisions between the drops.

It is interesting to observe the different types of pinch-off that occur in the two low frequency forcing cases. In Fig. 6b, the smaller drop goes through filling then pinching stages similar to the larger drop. The shape of the

pinch-off region differs, however. It appears that an approaching maximum in jet diameter broadens the cone upstream of the pinch-off and hence affects the angles in the pinch-off zone. Similar behavior is observed in Fig. 6a (second, third, and fourth images) where a maximum in jet diameter lies upstream of a local minimum. In the fourth image of the sequence, which occurs just after a pinch-off, the angles in the region appear inverted compared with those measured in Fig. 5. These examples show that local variations in the jet diameter (caused by variations in velocity) can have a strong effect on the shape of the pinch-off region.

4.3

Fluid combination 2

Figure 7 depicts the drop formation for $Re = 50$, $Fr = 0.27$, and fluid combination 2 ($\mu_i/\mu_o = 0.0077$). (Note that in this and the subsequent figures, the magnification is approximately one half of the magnification in Fig. 6.) Other than the viscosity ratio, the parameters are the same as those discussed above for fluid combination 1. The change in viscosity ratio causes significant differences in both drop formation and flow propagation. At this Re , the natural flow for fluid combination 1 yielded a stable jet that did not pinch off before reaching the reservoir interface ($20 D$ from the nozzle). In contrast, Fig. 7a shows that the natural flow for fluid combination 2 results in drops forming near the nozzle. The drop formation was similar to the dripping mode observed at low Re for fluid combination 1 (Fig. 2d). The drops in this case have a nominal diameter of $1.7 D$, which is considerably larger than even the largest forced drops at this Re for fluid combination 1 (Fig. 6). In this case, the natural drop size and spacing were uniform and repeatable. This is in contrast to the irregular drop characteristics for the natural flow at lower Re in fluid combination 1 (Fig. 2).

In this case, drops form closer to the nozzle than for fluid combination 1 because the high viscosity of the ambient fluid acts to retard the downward flow (regardless of whether it comes from inertia or buoyancy). In the case of low ambient viscosity, buoyancy is large enough to overcome the opposing drag force (as evidenced by the acceleration of the jet fluid and reduction in jet diameter as the fluid moved downward). The subsequent drop diameter is related to the local jet diameter where instabil-

ities initiate. In Fig. 7a, the high ambient viscosity and resulting drag force prevent a jet from developing. Instead, instabilities develop close to the nozzle, and larger drops form. The drops observed in the dripping mode in Fig. 2d are also considerably larger than those formed downstream of a jet (Fig. 2a, b, c)). Those drops are nevertheless smaller than the ones observed for fluid combination 2. A momentum balance on a gravity-driven dripping flow shows explicitly that increased drag caused by larger outer viscosity should result in larger drops.

Brenner et al. (1997) observed that for liquid drops forming in air, the shape just before pinch-off was dramatically affected by the liquid (inner fluid) viscosity. In the current example, it is clear that the ambient (outer fluid) viscosity also plays an important role in determining the shape approaching pinch-off. In particular, the angle defined by the drop and jet column connection was much more symmetric (i.e., $\beta_u \approx \beta_d$) than for fluid combination 1 (compare Fig. 7a to Fig. 4). This result, as well as additional flow visualization (of lower quality and therefore not shown) on a fluid combination with viscosity ratio of 1, plus the result of Lister and Stone (1998) suggests that, in the absence of compounding effects like subharmonic forcing, β_d increases with outer fluid velocity and β_u decreases. When put in terms of viscosity ratio, this is an extension of the same trend observed by Brenner et al. (1997).

The fundamental pinch-off mode (a single isolated drop forming during each cycle) occurred at a much lower Strouhal number than for fluid combination 1, which is consistent with the larger drop volume. Figure 7b shows forced flow at $St = 0.3$. This forcing frequency was a factor of 10 smaller than the forcing frequency for fluid combination 1 ($St = 3.1$, Fig. 3). By comparing the two images in Fig. 7, one can see that the natural drop frequency and size are very similar to this forced case. The drop propagation velocity and Reynolds number, Re_{drop} , for this case are $1.4 U_e$ and 0.7 , respectively. In this creeping flow regime, the outer fluid streamlines should be attached at the rear of the drop. As in fluid combination 1, however, the images indicate a mild flattening at the rear of each drop, again suggesting an overshoot resulting from the pinch-off process.

Increasing the flow rate to $Re = 180$ and $Fr = 1.0$ led to larger drops as shown in Fig. 8. The diameter of the drops was roughly $2.2 D$. As in other cases, the drop was initially a prolate spheroid, but it evolved into an asymmetric oblate spheroid within a few nozzle diameters. One very interesting aspect of this flow is the unusual pinch-off mechanism. Close examination of the image reveals very thin filaments of water-glycerin connecting what appear,

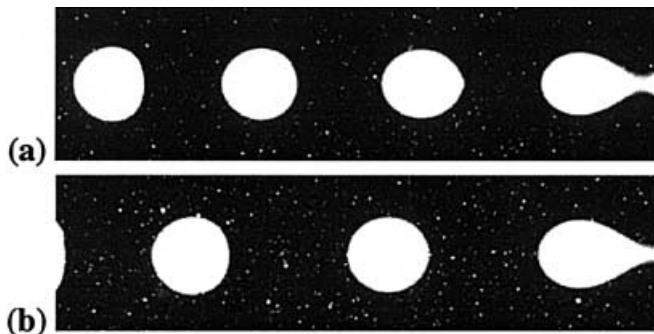


Fig. 7a, b. $Re = 50$, $Fr = 0.27$, fluid combination 2, a natural jet, b forced at $St = 0.3$. Length of each image is $13.5 D$



Fig. 8. Natural jet at $Re = 180$, $Fr = 1.0$, fluid combination 2. Length of each image is $13.5 D$

at first glance, to be independent drops. These filaments remained until at least $10 D$ downstream of the nozzle. Zhang and Basaran (1995) and Brenner et al. (1997) observed thin filaments for high viscosity liquids in air, but in those cases, the upstream structure was conically shaped with a larger value of β_u .

Increasing the flow rate further to $Re = 430$ and $Fr = 2.4$ changed the flow characteristics dramatically. The axisymmetry of the jet column was broken, and the jet wandered erratically from the center axis. (A stable axisymmetric jet could not be achieved for any Re attempted.) Bisecting the three-dimensional jet motion with the laser sheet led to the images in Fig. 9 (the images were taken approximately 0.4 s apart). The segments that appear to be disconnected are actually connected by jet fluid outside of the laser sheet plane. There was no evidence of pinch-off or drop formation for this set of parameters.

5

Conclusions

The behavior of liquid-liquid mixtures with significant interfacial tension was investigated by injecting water-glycerin solutions into ambients of immiscible Dow Corning 200 fluid. The index of refraction of the fluids was matched in order to examine the flow without optical distortion. Phase-locked LIF images of dye in the water-glycerin solution revealed the evolution of the interface shape through pinch-off as well as the size, shape, spacing,

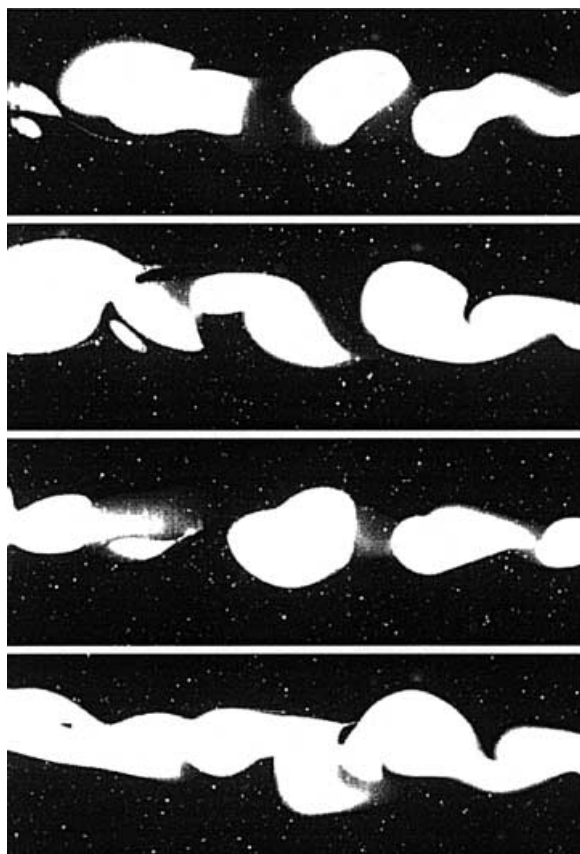


Fig. 9. Natural jet at $Re = 430$, $Fr = 2.4$, fluid combination 2. Length of each image is $13.5 D$

and speed of the downstream drops. Two fluid combinations with vastly different viscosity ratios were examined in the experiments.

For fluid combination 1, the forcing frequency had a dramatic effect on the pinch-off dynamics. For $Re = 50$, $Fr = 0.26$, the natural jet was stable over the length of the ambient reservoir. When the flow was forced at $St = 3.1$, instability waves formed on the jet column, and the jet pinched off into a single discrete drop during each forcing cycle. Initially the drops resembled prolate spheroids, but within a few nozzle diameters they evolved into asymmetric oblate spheroids. Over the downstream range viewed, the rear of the oblate spheroid was slightly flatter than the front for all the drops observed in these experiments. Decreasing the forcing frequency caused the formation of multiple drops of varying size within a single forcing cycle. The pinch-off dynamics were affected also, as observed by variations in interface angle between drops and the jet column just before pinch-off. Buoyant forces caused the larger drops to propagate more rapidly than and eventually catch up to smaller ones. The drops did not coalesce, but rather moved together downstream.

The viscosity ratio between the fluids had a strong effect on the flow regime and pinch-off characteristics. For all other parameters remaining essentially equal, the jet demonstrated alternative behavior when the ambient viscosity was increased by a factor of 20. One difference was that the natural flow pinched off into drops close to the nozzle. The total interface angle between the drop and jet column was smaller than in fluid combination 1 and more symmetric (upstream to downstream). In addition, the size and spacing of the drops were considerably larger for fluid combination 2. Increasing the flow rate led to even larger drops. At $Re = 180$, $Fr = 1.0$, a very thin filament of jet fluid was observed connecting the drops over a range up to ten diameters below the nozzle. For larger flow rates, a jet developed, but it followed an erratic helical motion and did not pinch off into drops.

References

- Batchelor GK (1967) An introduction to fluid dynamics. Cambridge University Press, Cambridge
- Brenner MP; Eggers J; Joseph K; Nagel SR; Shi XD (1997) Breakdown of scaling in droplet fission at high Reynolds number. *Phys Fluids* 9: 1573-1590
- Clift R; Grace JR; Weber ME (1978) Bubbles, drops and particles. Academic Press, New York
- Cristini V; Blawdziewicz J; Loewenberg M (1998) Drop breakup in three-dimensional viscous flows. *Phys Fluids* 10: 1781-1783
- Joseph DD; Arney MS; Gillberg G; Hu H; Hultman D; Verdier C; Vinagre HMT (1992) A spinning drop tensioextensometer. *J Rheol* 36: 621-662
- Kitamura Y; Mishima H; Takahashi T (1982) Stability of jets in liquid-liquid systems. *Can J Chem Eng* 60: 723
- Lister JR; Stone HA (1998) Capillary breakup of a viscous thread surrounded by another viscous fluid. *Phys Fluids* 10: 2758-2764
- Meister BJ; Scheele GF (1969a) Prediction of jet length in immiscible liquid systems. *AIChE J* 15: 689-699
- Meister BJ; Scheele GF (1969b) Drop formation from cylindrical jets in immiscible liquid systems. *AIChE J* 15: 700-706
- Richards JR; Lenhoff AM; Beris AN (1994) Dynamic breakup of liquid-liquid jets. *Phys Fluids* 6: 2640

- Richards JR; Scheele GF** (1985) Measurement of laminar jet velocity distributions in liquid-liquid systems using flash photolysis. *Chem Eng Commum* 36: 73
- Scheele GF; Meister BJ** (1968) Drop formation at low velocities in liquid-liquid systems: Part 1. Prediction of drop volume. *AI-ChE J* 14: 9
- Skelland AHP; Johnson KR** (1974) Jet break-up in liquid-liquid systems. *Can J Chem Eng* 52: 732
- Skelland AHP; Walker PG** (1989) The effects of surface active agents on jet breakup in liquid-liquid systems. *Can J Chem Eng* 67: 762-70
- Stone; HA** (1994) Dynamics of drop deformation and breakup in viscous fluids. *Ann Rev Fluid Mech* 26: 65
- Tadrist L; Alaoui EKO; Occelli R; Pantaloni J** (1991) Experimental study of a liquid jet flowing into another immiscible liquid: a local analysis of the interface. *Exp Fluids* 12: 67
- Vijayan S; Ponter AB; Jeffreys GV** (1975) The effect of a relative boundary velocity on single drop/interface coalescence times. *Chem Eng J* 10: 145
- Zhang DF; Stone HA** (1997) Drop formation in viscous flow at a vertical capillary tube. *Phys Fluids* 9: 2234
- Zhang X; Basaran OA** (1995) An experimental study of dynamics of drop formation. *Phys Fluids* 7: 1184